





# Human FAM111A inhibits vaccinia virus replication by degrading viral protein I3 and is antagonized by poxvirus host range factor SPI-1

Junda Zhu<sup>a,1</sup>, Xintao Gao<sup>b,1</sup>, Yijing Li<sup>c</sup>, Zihui Zhang<sup>a</sup>, Shijie Xie<sup>a</sup>, Shuning Ren<sup>a</sup>, Yarui Li<sup>a</sup>, Hua Li<sup>a</sup>, Kang Niu<sup>a</sup>, Shufang Fu<sup>a</sup>, Yining Deng<sup>a</sup>, Yinü Li<sup>b</sup>, Bernard Moss<sup>d</sup> , Wenxue Wu<sup>a,2</sup>, and Chen Peng<sup>a,2</sup> 

Edited by Geoffrey L. Smith, University of Oxford, Oxford, United Kingdom; received March 17, 2023; accepted July 10, 2023 by Editorial Board Member Xiang-Jin Meng

Zoonotic poxviruses such as mpox virus (MPXV) continue to threaten public health safety since the eradication of smallpox. Vaccinia virus (VACV), the prototypic poxvirus used as the vaccine strain for smallpox eradication, is the best-characterized member of the poxvirus family. VACV encodes a serine protease inhibitor 1 (SPI-1) conserved in all orthopoxviruses, which has been recognized as a host range factor for modified VACV Ankara (MVA), an approved smallpox vaccine and a promising vaccine vector. FAM111A (family with sequence similarity 111 member A), a nuclear protein that regulates host DNA replication, was shown to restrict the replication of a VACV SPI-1 deletion mutant (VACV- $\Delta$ SPI-1) in human cells. Nevertheless, the detailed antiviral mechanisms of FAM111A were unresolved. Here, we show that FAM111A is a potent restriction factor for VACV- $\Delta$ SPI-1 and MVA. Deletion of FAM111A rescued the replication of MVA and VACV- $\Delta$ SPI-1 and overexpression of FAM111A significantly reduced viral DNA replication and virus titers but did not affect viral early gene expression. The antiviral effect of FAM111A necessitated its trypsin-like protease domain and DNA-binding domain but not the PCNA-interacting motif. We further identified that FAM111A translocated into the cytoplasm upon VACV infection by degrading the nuclear pore complex via its protease activity, interacted with VACV DNA-binding protein I3, and promoted I3 degradation through autophagy. Moreover, SPI-1 from VACV, MPXV, or lumpy skin disease virus was able to antagonize FAM111A by prohibiting its nuclear export. Our findings reveal the detailed mechanism by which FAM111A inhibits VACV and provide explanations for the immune evasive function of VACV SPI-1.

FAM111A | poxvirus | modified vaccinia virus Ankara (MVA) | antiviral response | virus-host interaction

During their coevolution, viruses and their hosts have evolved numerous strategies to antagonize each other. Upon viral infection, cells initiate various programs, such as the induction of type I interferons and the expression of an armory of antiviral factors that can restrict viral invasion, gene expression, DNA replication, and virion assembly. More recent findings point to the fact that some host defense factors are multifunctional and can display potent antiviral activity in a way that is distinct from their regular cellular functions (1–4). One such example is FAM111A (family with sequence similarity 111 member A), a protein with a fully functional trypsin-like C-terminal protease domain that is found exclusively in mammals (5). FAM111A prevents replication forks from stalling via its protease domain and disease-associated mutants display aberrant nuclear morphology due to the disruption of the nuclear pore complex (NPC) as a result of its hyperactive protease activity (6, 7). Recent studies have shown that FAM111A also has antiviral functions. Fine et al. identified FAM111A as a host restriction factor for simian virus 40 (SV40) and showed that FAM111A was specifically targeted by the C-terminal region of SV40 large T (LT) antigen (6, 8, 9). In addition, Panda et al. identified FAM111A as a restriction factor for a vaccinia virus (VACV) host-range mutant (VACV- $\Delta$ SPI-1) through genome-wide RNAi screening (10). However, the detailed mechanisms by which the nuclear protein FAM111A restricts viral infections, especially infections of poxviruses that replicate exclusively in the cytoplasm, remain largely elusive.

Poxviruses are large cytoplasmic DNA viruses and as a family can infect a wide variety of different animal species (11). The most notorious members of the poxvirus family include variola virus, the causative agent of smallpox, and mpox virus (MPXV), which is responsible for the recent global outbreaks of mpox (12–15). VACV was the vaccine strain used for the eradication of smallpox and is also the prototypic poxvirus that is best characterized (16, 17). The genome of VACV encodes for more than 200 proteins, nearly half

## Significance

FAM111A (family with sequence similarity 111 member A) is a nuclear trypsin-like peptidase that regulates DNA replication in mammals. Recent research has shown that FAM111A restricts the replication of vaccinia virus lacking serine protease inhibitor 1 (VACV- $\Delta$ SPI-1), although the underlying antiviral mechanism remains incompletely characterized. Here, we show that FAM111A is activated upon virus infection via the cGAS-STING signaling pathway and inhibits viral infection by specifically targeting its DNA-binding protein I3 for autophagic degradation. Moreover, we reveal that SPI-1 from various poxviruses with different host ranges can antagonize human FAM111A's antiviral activity by inhibiting its peptidase function. Collectively, these findings provide a detailed insight into the antiviral mechanism of FAM111A and illustrate how VACV-SPI-1 evades its antiviral activity.

The authors declare no competing interest.

This article is a PNAS Direct Submission. G.L.S. is a guest editor invited by the Editorial Board.

Copyright © 2023 the Author(s). Published by PNAS. This article is distributed under [Creative Commons Attribution-NonCommercial-NoDerivatives License 4.0 \(CC BY-NC-ND\)](https://creativecommons.org/licenses/by-nc-nd/4.0/).

<sup>1</sup>J.Z. and X.G. contributed equally to this work.

<sup>2</sup>To whom correspondence may be addressed. Email: wuwenxue@cau.edu.cn or pengchenea@cau.edu.cn.

This article contains supporting information online at <https://www.pnas.org/lookup/suppl/doi:10.1073/pnas.2304242120/-/DCSupplemental>.

Published August 22, 2023.

of which are involved in host-virus interactions and a third of them responsible for evading host antiviral defenses (11). VACV encodes three serine protease inhibitors (SPI-1, SPI-2, and SPI-3). Deletion of SPI-1 from VACV caused a host range defect that can be rescued by depletion of FAM111A (10). Moreover, insertion of SPI-1 into MVA (modified VACV Ankara), the highly attenuated vaccine strain unable to replicate in most mammalian cells, was able to rescue MVA's replicative capability in certain mammalian cells such as BS-C-1 and MRC-5 (18, 19), although whether MVA can also be rescued by depletion of FAM111A is not known.

Here, we demonstrated that FAM111A, a component of the cellular replication fork primarily localized in the nucleus under normal conditions, was translocated into the cytoplasm in MVA-infected cells upon the activation of the cGAS-STING signaling pathway during MVA infection. The export of FAM111A necessitated the disruption of NPC via its protease activity. Cytoplasmic FAM111A colocalized with viral DNA-binding protein I3 and mediated its degradation through autophagy, leading to the arrest of viral DNA replication, postreplicative protein expression, and eventually virus replication. During VACV infection, SPI-1 entered the nucleus of infected cells and prevented the nuclear export of FAM111A by inhibiting the peptidase activity of the latter, and a functional SPI-1 reactive-site loop (RSL) was indispensable for this inhibitory effect (20). Our findings uncover the molecular mechanism by which FAM111A suppresses VACV replication and demonstrate the mode of action of SPI-1 in antagonizing the antiviral function of FAM111A.

## Results

### FAM111A Is a Host Restriction Factor for VACV Lacking SPI-1.

To verify the antiviral effect of FAM111A, we cloned human FAM111A into a mammalian expression vector and expressed it ectopically in human A549 cells before infecting the cells with MVA, MVA engineered to express SPI-1, or/and a second

host-range factor C16 (MVA+SPI-1, MVA+SPI-1/C16), VACV-WR (Western Reserve strain) or VACV- $\Delta$ SPI-1 (21). We examined the expression of viral proteins by western blotting with anti-VACV rabbit antiserum and virus replication by plaque assay. Overexpression of transfected FAM111A DNA was demonstrated with an anti-FAM111A antibody (Fig. 1A). Even though the expression of SPI-1 increased MVA protein synthesis, it was severely reduced by overexpression of FAM111A (Fig. 1A). FAM111A also reduced protein synthesis by MVA+SPI-1/C16, though to a lesser extent. Although VACV-WR appeared relatively resistant to FAM111A, viral protein synthesis induced by VACV with a deleted SPI-1 (VACV- $\Delta$ SPI-1) was diminished as much as MVA (Fig. 1A). In conformity with the results of western blotting, overexpressing FAM111A significantly attenuated the replication of VACV in A549 cells, and the effects were more pronounced for VACV- $\Delta$ SPI-1 and MVA (Fig. 1B). The antiviral effect of FAM111A was enhanced as we increased the amount of FAM111A DNA transfected in MVA and VACV- $\Delta$ SPI-1-infected cells (SI Appendix, Fig. S1A). To test the role of FAM111A on viral DNA replication, we examined the abundance of viral DNA using a set of primers for the VACV E11 open reading frame in cells transfected with FAM111A and infected with MVA, VACV-WR and their recombinants indicated in the figure at 3 PFU/cell (Fig. 1C), and the blockage of viral DNA replication was observed in the presence of FAM111A (22). In agreement with the above results, viral DNA loads were decreased significantly in both MVA and VACV- $\Delta$ SPI-1-infected cells in an FAM111A dose-dependent manner (SI Appendix, Fig. S1B), further confirming the FAM111A blockade of viral DNA replication.

Next, we determined whether depletion of endogenous FAM111A could relieve the replication of VACV lacking SPI-1. We first transiently knocked down the expression of FAM111A by transfecting A549 cells with siFAM111A or the negative control siNC. The expression of viral proteins determined by anti-VACV antiserum (SI Appendix, Fig. S1C), virus titers (SI Appendix, Fig. S1D), and viral DNA loads (SI Appendix, Fig. S1E) were much higher in cells

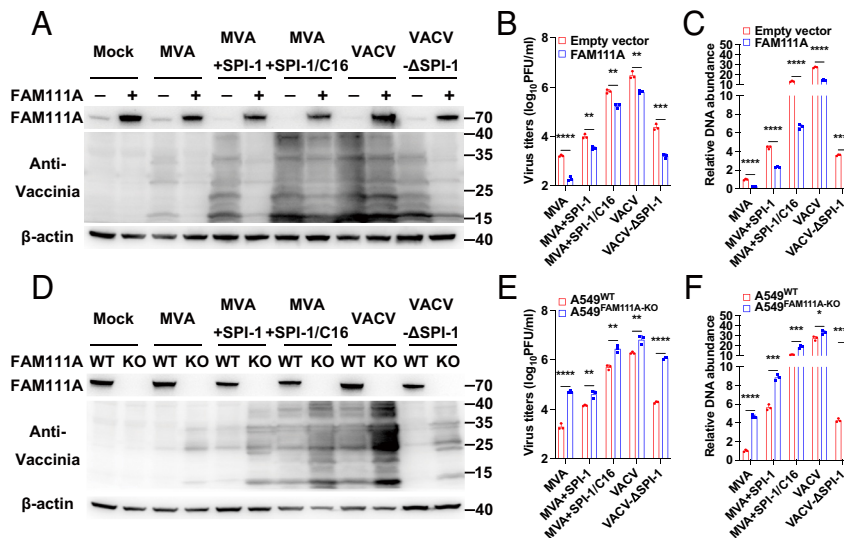


**Fig. 1.** FAM111A prohibits the replication of vaccinia viruses lacking SPI-1 in A549 cells. (A, B, and C) A549 cells were transfected with FAM111A for 24 h and then infected with viruses indicated in the figures at 0.3 PFU/cell. Cell lysates were analyzed by SDS-PAGE and western blotting at 12 hpi (A); Indicated cells were infected at 0.03 PFU/cell. Viruses were harvested at 24 hpi and quantified by plaque assay on DF-1 (MVA, MVA+SPI-1, and MVA+SPI-1/C16) or BS-C-1 cells (VACV, VACV- $\Delta$ SPI-1) (B); Indicated cells were infected at 3 PFU/cell. Total cellular DNA was harvested at 6 hpi, and viral genomic DNA levels were determined by RT-qPCR using primers for E11 ORF (C). (D–F) Human A549<sup>WT</sup> or A549<sup>FAM111A-KO</sup> cells were infected with the viruses described above at 0.3 PFU/cell. Cell lysates were analyzed by SDS-PAGE and western blotting (D); Indicated cells were infected at 0.03 PFU/cell. Viruses were harvested at 24 hpi and quantified by plaque assay (E); Indicated cells were infected at 3 PFU/cell. Total DNA was harvested at 6 hpi, and viral genomic DNA levels were determined by RT-qPCR (F). Data in B, C, E, and F represent the mean values  $\pm$  SD of three independent experiments. Data in A–F are representative of three independent experiments. Statistics: ns, not significant; \* $P < 0.05$ ; \*\* $P < 0.01$ ; \*\*\* $P < 0.001$ ; \*\*\*\* $P < 0.0001$  by two-sided Student's  $t$  test.

transfected with siFAM111A than in those transfected with only siNC as a negative control, and the comparison was more dramatic in MVA and VACV- $\Delta$ SPI-1-infected cells than in cells infected with SPI-1-expressing viruses. To further confirm our findings, A549<sup>FAM111A-KO</sup> cell lines were generated using CRISPR-Cas9 technology with sgRNA targeting the 5' region of FAM111A. The depletion of the protein was verified by western blotting analysis (SI Appendix, Fig. S2) and was further confirmed by Sanger sequencing. We infected A549<sup>WT</sup> and A549<sup>FAM111A-KO</sup> cells with the above-described viruses and examined the expression of viral protein synthesis, DNA abundance, and virus titers using the methods described. Depletion of FAM111A significantly increased viral protein synthesis (Fig. 1D), virus titers (Fig. 1E), and viral DNA loads (Fig. 1F) for MVA and VACV- $\Delta$ SPI-1. However, replication of VACV-WT was not severely affected by FAM111A depletion. Notably, even though VACV- $\Delta$ SPI-1 replicated better in FAM111A-KO cells than in WT cells, the titer was still lower than what VACV-WT could achieve in either A549<sup>WT</sup> or A549<sup>FAM111A-KO</sup> cells, indicating that additional restricting factors may exist for VACV- $\Delta$ SPI-1.

Previous studies have indicated that SPI-1 had only a small effect on MVA replication in monkey BS-C-1 cells and was unnecessary for replication in chicken DF-1 cells (19). To test whether FAM111A is a species-specific host restriction factor, we transfected monkey BS-C-1 cells and chicken DF-1 cells with human FAM111A DNA and found human FAM111A failed to restrict replication of an MVA expressing SPI-1 and C16 (MVA 47.1) in BS-C-1 cells or MVA and MVA+SPI-1 in DF-1 cells, indicating that the antiviral function of FAM111A may require other unknown cellular factors that could be species-specific and are absent in nonhuman cells (SI Appendix, Fig. S3).

To determine whether viral infections influence the amount of FAM111A, proteins were collected from MVA- or VACV-infected human A549 cells for western blotting analysis, and no change in FAM111A was observed after virus infection (SI Appendix, Fig. S4). In summary, our results illustrated that FAM111A was a restriction factor for MVA and VACV- $\Delta$ SPI-1 and is antagonized by SPI-1.

**Inhibition of VACV- $\Delta$ SPI-1 and MVA by FAM111A Requires Its Functional Protease Domain.** The C-terminal domain of FAM111A contains a trypsin-like motif that constitutes a catalytic triad consisting of His385, Aps439, and Ser541 and is highly conserved among mammals (23). Mutation of S541A inactivates the enzymatic function of FAM111A, while mutation of R569H represents a hyperactive mutation observed in patients diagnosed with Kenny–Caffey syndrome and osteocraniostenosis exhibiting heightened self-cleavage activity (23). To assess whether FAM111A's antiviral effect is dependent on its protease activity, we generated vectors containing a loss-of-function mutant FAM111A<sup>S541A</sup>, a hyperactive mutant FAM111A<sup>R569H</sup>, or a double mutant FAM111A<sup>S541A+R569H</sup> that was previously shown to behave like a loss-of-function mutant (Fig. 2A). When transfected into human cells, FAM111A<sup>S541A</sup> and FAM111A<sup>S541A+R569H</sup> mutants caused accumulation of the protein comparing to FAM111A<sup>WT</sup> (Fig. 2B), a result of decreased self-cleavage activity (7). The hyperactive mutant FAM111A<sup>R569H</sup> was expressed at a lower level compared to FAM111A<sup>WT</sup>, possibly due to excessive self-cleavage rather than proteasome-mediated degradation as the addition of MG132 (20  $\mu$ M), a proteasome inhibitor, showed no effect on FAM111A protein levels (Fig. 2C). These results confirmed that the mutations indeed altered its protease activity. Next, A549 cells transfected with either FAM111A<sup>WT</sup> or mutated

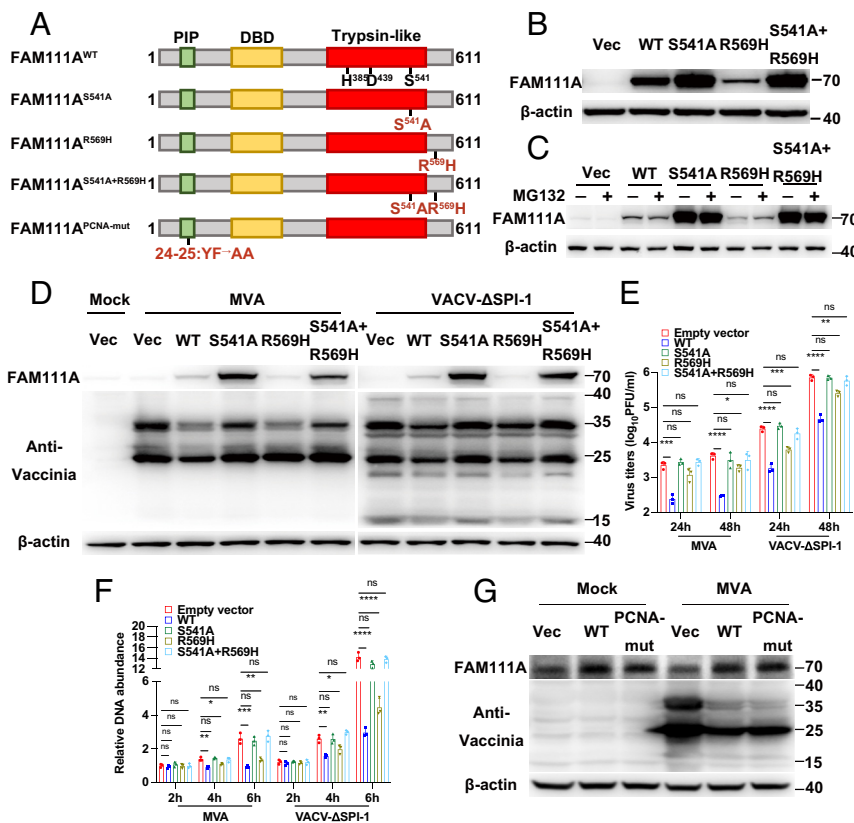


**Fig. 2.** The antiviral effect of FAM111A is dependent on its protease activity. (A) Schematic of the protein structures of FAM111A with defined domains, the trypsin catalytic triplet mutants, and PCNA interaction domain mutant. Trypsin-like: the protease domain. PIP box: PCNA interaction domain. DBD: DBD. (B and C) Human A549 cells were transfected with FAM111A<sup>WT</sup>, FAM111A<sup>S541A</sup>, FAM111A<sup>R569H</sup>, or FAM111A<sup>S541A+R569H</sup> for 24 h in the presence or absence of MG132. Cell lysates were collected and analyzed by SDS-PAGE and western blotting. (D–F) Human A549 cells were transfected with FAM111A<sup>WT</sup>, FAM111A<sup>S541A</sup>, FAM111A<sup>R569H</sup>, or FAM111A<sup>S541A+R569H</sup> for 24 h and then infected with MVA or VACV- $\Delta$ SPI-1 at 0.3 PFU/cell. Cell lysates were analyzed by SDS-PAGE and western blotting at 12 hpi (D); Indicated cells were infected with MVA at 0.03 PFU/cell. Viruses were harvested at 24 hpi and quantified by plaque assay (E); Indicated cells were infected with MVA or VACV- $\Delta$ SPI-1 at 3 PFU/cell. Total DNA was harvested at 6 hpi, and viral genomic DNA levels were determined by RT-qPCR (F). (G) Human A549 cells were transfected with FAM111A<sup>WT</sup> or FAM111A<sup>PCNA-mut</sup> for 24 h and then infected with MVA at 0.3 PFU/cell. Cell lysates were harvested and analyzed with SDS-PAGE and western blotting. Data in E and F represent the mean values  $\pm$  SD of three independent experiments. Data in B–G are representative of three independent experiments. Statistics: ns, not significant; \* $P$  < 0.05; \*\* $P$  < 0.01; \*\*\* $P$  < 0.001; \*\*\*\* $P$  < 0.0001 by two-sided Student's  $t$  test.

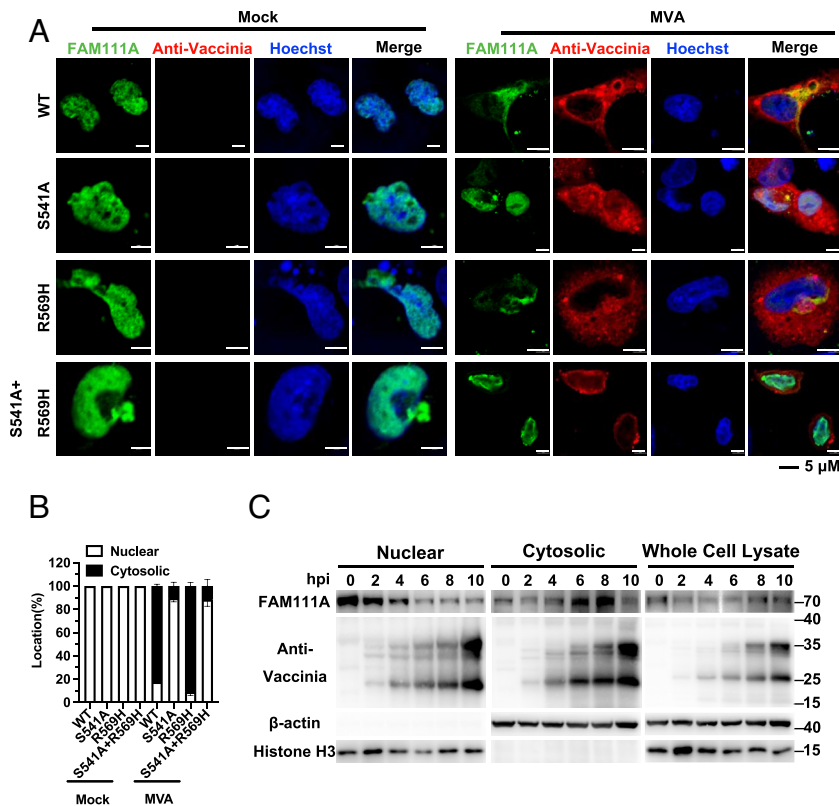


**Fig. 3.** MVA infection prompts protease-dependent relocalization of FAM111A. (A and B) Human A549 cells plated on coverslips were transfected with FAM111A<sup>WT</sup>, FAM111A<sup>S541A</sup>, FAM111A<sup>R569H</sup>, or FAM111A<sup>S541A+R569H</sup> for 24 h and then infected with MVA at 3 PFU/cell. After 12 h, cells were fixed, permeabilized, blocked, and stained with primary antibodies to FAM111A and rabbit antiserum to VACV followed by fluorescent conjugated secondary antibodies. Hoechst was used to stain DNA (A); The confocal analyses were performed in triplicates and the localization of FAM111A was quantified in 100 randomly selected cells, and bars represent mean values  $\pm$  SD (B). (C) Human A549 cells were infected with MVA at 3 PFU/cell, and protein was harvested at time points indicated in the figure. Protein components in the nucleus and cytosol were separated by nuclear and cytoplasmic protein extraction kit and analyzed by SDS-PAGE and western blotting. Anti- $\beta$ -actin and anti-histone H3 were used for cytosolic and nuclear loading controls, respectively. Data in B represent the mean values  $\pm$  SD of three independent experiments. Data in A and C are representative of three independent experiments.

FAM111A DNAs were infected with MVA or VACV- $\Delta$ SPI-1, and viral protein synthesis, virus growth, and DNA replication were monitored. The results showed that the reduction of VACV protein caused by overexpressing FAM111A was eliminated when the enzymatic activity was disrupted through S541 mutation, even though the mutants without a functional protease domain were expressed at much higher levels (Fig. 2D). It is worth noting that the hyperactive mutation FAM111A<sup>R569H</sup> did not further decrease viral protein synthesis compared to FAM111A<sup>WT</sup>, which may be the result of low FAM111A accumulation due to excessive self-cleavage. In addition, FAM111As with loss-of-function mutations were no longer able to suppress virus replication (Fig. 2E) and viral DNA replication (Fig. 2F) in A549 cells, while the gain-of-function mutation did not show a significantly altered antiviral activity compared to FAM111A<sup>WT</sup>. As the proliferating cell nuclear antigen (PCNA) interaction motif is required for its physiological function for host DNA replication, we generated a mutant that contained mutations in the PIP box (Fig. 2A) and found the loss of PCNA binding did not compromise the antiviral function of FAM111A (Fig. 2G). These results demonstrated that the protease activity of FAM111A was indispensable for its antiviral function.

#### MVA Infection Leads to the Nuclear Export of FAM111A.

Unlike most DNA viruses, poxvirus replication is restricted to the cytoplasm of infected cells. Therefore, we considered that FAM111A, a protein found in the nucleus under normal conditions, would have to be exported to the cytosol to exert its antiviral effect. To determine whether viral infection triggers changes in the subcellular localization of FAM111A, A549 cells plated on coverslips were mock-infected or infected with MVA and the subcellular localization of FAM111A was determined by immunofluorescence using anti-FAM111A antibodies and Hoechst dye that could stain nucleus and virus factories. In mock-infected cells, FAM111A was exclusively found in the nucleus and the

hyperactive mutation of FAM111A caused aberrant morphology of the nucleus, consistent with a previous report (Fig. 3A) (6). When infected with MVA, however, FAM111A<sup>WT</sup> was found primarily in the cytosol (Fig. 3A). In contrast, the two FAM111A mutants with inactivated protease domain failed to translocate and remained in the nucleus. FAM111A<sup>R569H</sup>, on the other hand, was also found predominantly in the cytosol but with a more concentrated distribution close to the viral factories (Fig. 3A). The subcellular localization of FAM111A and its mutants upon viral infection was also quantified and the results are shown in Fig. 3B. We further isolated nuclear and cytosolic proteins and examined the abundance of FAM111A in each fraction and were able to confirm the nuclear decrease of FAM111A upon MVA infection in a time-dependent manner (Fig. 3C). The above experiments were repeated in HeLa cells, and the results were consistent (SI Appendix, Fig. S5). These findings illustrated that MVA triggers the translocation of FAM111A into the cytoplasm, and this process relies on the normal catalytic activity of FAM111A.

#### MVA Infection Triggers FAM111A-Mediated NPC Degradation through Activation of the cGAS-STING Signaling Pathway.

A previous report showed that overexpression of FAM111A could cause loss of nuclear barrier function of the NPC (6). We reasoned that the nuclear export of FAM111A may be achieved through the destruction of NPC by FAM111A's protease activity. To test this hypothesis, A549 cells were transfected with FAM111A DNA or the loss-of-function and hyperactive mutants, and Mab414 was used to stain NPC for confocal microscopic analysis. As expected, transfection of FAM111A<sup>WT</sup> and FAM111A<sup>R569H</sup> DNAs disrupted NPC structure, and FAM111A<sup>S541A</sup> and FAM111A<sup>S541A+R569H</sup> showed no such effect (SI Appendix, Fig. S6A). In addition, NUP62, a core component of the NPC was found degraded by FAM111A (SI Appendix, Fig. S6B). To test whether endogenous FAM111A could degrade NPC upon viral infection, A549 cells

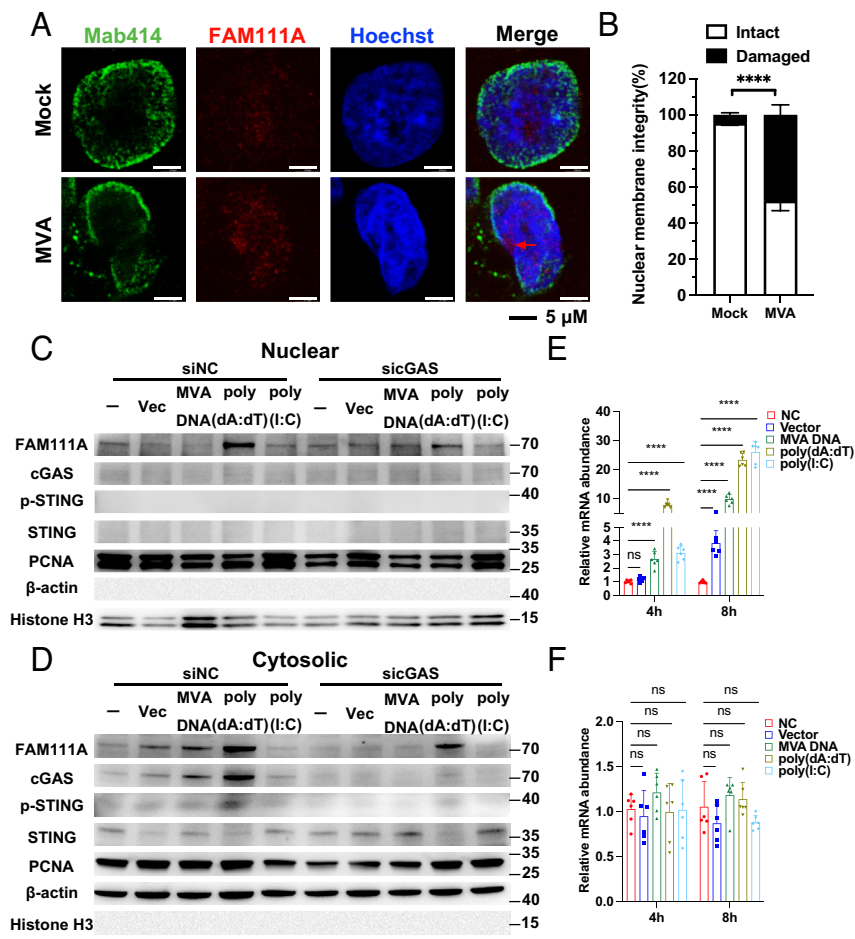


**Fig. 4.** MVA infection induces NPC degradation by FAM111A which is enabled by the activation of the cGAS-STING signaling pathway. (A and B) Human A549 cells were mock-infected or infected with MVA at 3 PFU/cell. After 6 h, cells were fixed, permeabilized, blocked, and stained with primary antibodies to Mab414 and FAM111A followed by fluorescent conjugated secondary antibodies. The red arrow indicates FAM111A accumulated near the nuclear membrane after MVA infection, and the NPC destroyed by it. Hoechst was used to stain DNA (A); The confocal analyses were performed in triplicates and the localization of FAM111A was quantified in 100 randomly selected cells, and bars represent mean values  $\pm$  SD (B). (C and D) Human A549 cells were transfected with siNC or sicGAS for 48 h and then transfected with empty vector, DNA collected from MVA virus particles, poly(dA:dT), or poly(I:C) for 8 h. Nuclear and cytosolic proteins were separated using nuclear and cytoplasmic protein extraction kits and analyzed by SDS-PAGE and western blotting. Anti- $\beta$ -actin and anti-histone H3 were used for cytosolic and nuclear loading controls, respectively. (E and F) Human A549 cells (E) or 293T cells (F) were transfected with empty vector, DNA collected from MVA virus particles, poly(dA:dT), or poly(I:C) for 4 or 8 h. Total RNA was harvested, and mRNA levels of FAM111A were determined by RT-qPCR. Data in B, E, and F represent the mean values  $\pm$  SD of three independent experiments. Data in A–F are representative of three independent experiments. Statistics: ns, not significant; \*\*\*\* $P < 0.0001$  by two-sided Student's *t* test.

were mock-infected or infected with MVA at 3 PFU/cell for 6 h, and Mab414 antibody was used to examine NPC integrity by confocal microscopy. MVA infection led to disruption of the NPC in areas where FAM111A was concentrated (highlighted by red arrow), but the nuclear membrane was undisturbed in mock-infected cells (Fig. 4A). The results from the confocal microscopic analysis were also quantitated and were shown in Fig. 4B. These data revealed MVA infection triggered FAM111A-mediated NPC disruption and the subsequent nuclear export of FAM111A.

As the lifecycle of poxvirus occurs in the cytosol of infected cells, we wondered how FAM111A senses the invasion of MVA and initiates its migration to the cytosol. Cyclic GMP-AMP synthase (cGAS) is a crucial pattern recognition receptor activated by cytosolic DNA (24, 25). To determine whether cGAS is involved in FAM111A activation, we designed siRNA specific for cGAS and confirmed it was depressed efficiently (SI Appendix, Fig. S7). A549 cells transfected with siNC or sicGAS for 48 h were left untreated or transfected with an empty vector, extracted genomic DNA from MVA, poly(dA:dT), a repetitive synthetic dsDNA, or poly(I:C), a molecule used to simulate dsRNA. Total protein was collected, and components of nuclear and cytosolic proteins were isolated using the method described above. As shown in SI Appendix, Fig. S7, sicGAS was able to repress the expression of cGAS and phosphorylation of STING but had no effect on the expression of FAM111A, total STING, PCNA, or histone H3. Transfection of plasmid DNA, viral genomic DNA, or poly(dA:dT) all led to increased nuclear export of FAM111A while the transfection of poly(I:C) failed to do so (Fig. 4 C and D). Importantly, the cytosolic accumulation of FAM111A caused by transfection

of plasmid DNA or viral genomic DNA was largely reduced in cells transfected with sicGAS, indicating that the nuclear export of FAM111A was induced by dsDNA in the cytosol through the cGAS-STING signaling pathway. As transfection of DNA led to increased FAM111A, we aimed to determine whether this was achieved through transcriptional regulation by monitoring FAM111A mRNA upon nucleic acid stimulation. In A549 cells, FAM111A mRNA was up-regulated after transfection with plasmid DNA, poly(dA:dT) or poly(I:C) (Fig. 4E), while this phenomenon was not observed in 293T cells in which STING is naturally deficient (Fig. 4F). These results suggested that the expression and subcellular localization of FAM111A were indeed induced by the cGAS-STING signaling pathway, while the interferon signaling pathway induced by poly I:C is sufficient but not necessary for FAM111A activation (10).

**FAM111A Targets and Specifically Interacts with Virus DNA-Binding Protein 13.** The above experiments demonstrated that MVA infection induced nuclear export of FAM111A through the cGAS signaling pathway, and this process was achieved through NPC destruction. It was hence important to investigate how FAM111A exerted its antiviral activity. We first hypothesized that FAM111A could directly bind to and catalyze the degradation of certain viral proteins via its protease activity. We designed an experiment to pull down the viral interactome of FAM111A in MVA-infected cells and identify its components with mass spectrometric analysis (Fig. 5A). In this assay, VACV I3 showed the most significant increase in protein abundance between FAM111A-transfected and vector-transfected cells and was further

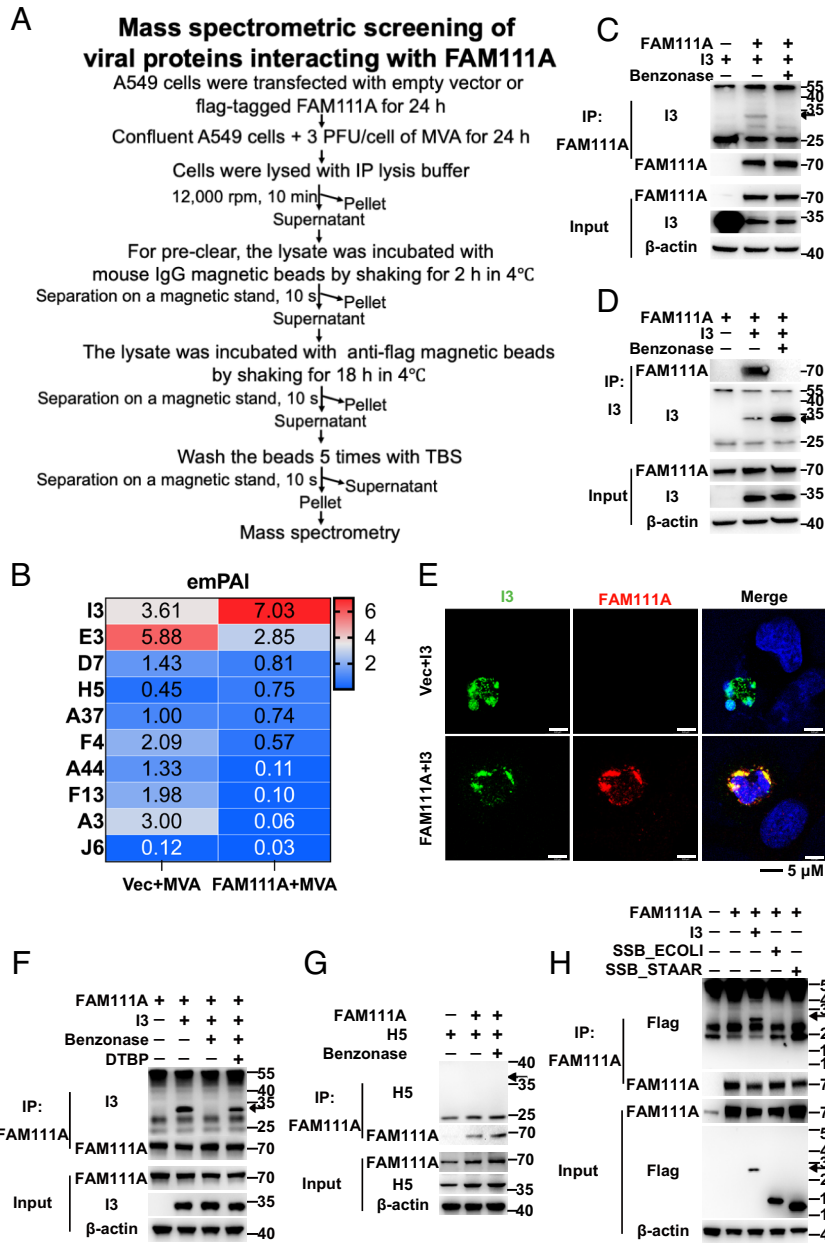


**Fig. 5.** FAM111A interacts directly with viral I3 in a DNA-dependent manner. (A) Schematic flow chart of mass spectrometric screening of MVA viral proteins interacting with FAM111A. (B) Mass spectrometry was used to identify the viral proteins that interacted with FAM111A. The relative content of viral proteins was expressed by the exponentially modified protein abundance index (emPAI). (C and D) Human A549 cells were cotransfected with myc-tagged FAM111A or flag-tagged I3 for 24 h. Cell lysates were first incubated with or without Benzonase (250 U/mL) at 37 °C for 20 min and then incubated with myc-/flag-conjugated beads at 4 °C for 18 h. Proteins were analyzed by SDS-PAGE and western blotting. (E) Human A549 cells were cotransfected with VACV-I3 and FAM111A for 24 h and infected with MVA at 3 PFU/cell. After 12 h, cells were fixed, permeabilized, blocked, and stained with primary antibodies to I3 and FAM111A followed by fluorescent conjugated secondary antibodies. Hoechst was used to stain DNA. (F) Human A549 cells were cotransfected with myc-tagged FAM111A or flag-tagged I3 for 24 h. Cell lysates were first incubated with or without DTBP (3 mM) on ice for 30 min and then incubated with or without Benzonase (250 U/mL) at 37 °C for 20 min. The method of co-IP and western blotting is as described above. (G) Human A549 cells were transfected with myc-tagged FAM111A or flag-tagged H5 for 24 h. The method of co-IP and western blotting is as described above. (H) Human A549 cells were transfected with myc-tagged FAM111A or flag-tagged I3, SSB\_ECOLI, or SSB\_STAAR for 24 h. The method of co-IP and western blotting is as described above. The arrow indicates the correct band size for I3 or H5, and the light chain or heavy chain antibody bands are at 25 kDa or 55 kDa, respectively. Data in C–H are representative of three independent experiments.

investigated as a putative target of FAM111A (Fig. 5B). VACV I3 contains a single-stranded DNA-binding domain (DBD), and deletion of I3 did not affect viral early protein synthesis or core disassembly but blocks DNA replication (26, 27). The interaction between FAM111A and I3 was first confirmed by coimmunoprecipitation (co-IP) analysis by using either FAM111A or I3 as the bait (Fig. 5C and D). To determine whether the interaction was DNA-dependent as FAM111A contains a double-stranded DBD, cell lysates were incubated with or without 250U/mL of benzonase, an endonuclease known to degrade all forms of DNA without base preference. The association of I3 and FAM111A disappeared when benzonase was added (Fig. 5C and D). As FAM111A contains a DBD and no discernible RNA binding motifs, we concluded that the interaction between FAM111A and I3 was DNA-dependent. Additional experiments were carried out to validate the colocalization of I3 and FAM111A within cells (Fig. 5E). A549 cells were cotransfected with vectors expressing viral I3 and human FAM111A for confocal microscopic analysis. As expected, I3 was associated with Hoechst-stained

virus factories in the cytoplasm of infected cells and the majority of FAM111A colocalized with I3 (Fig. 5E). Next, to determine whether FAM111A and I3 interacted with each other directly or indirectly through DNA binding, we performed co-IP analysis in the presence and absence of dimethyl dithiobispropionimidate (DTBP), a membrane permeable cross-linker (Fig. 5F). The association of FAM111A and I3 was no longer disrupted by benzonase after the addition of DTBP, suggesting that these two proteins engaged in direct interaction, with DNA serving merely as a means to bring them to close proximity. To further verify the specific interaction between FAM111A and I3, we tested whether FAM111A interacted with VACV H5, another virus protein known to bind DNA (Fig. 5G) or bacteria single-stranded DNA binding protein (SSB) from *Escherichia coli* (SSB\_ECOLI) or *Staphylococcus aureus* (SSB\_STAAR) (Fig. 5H) and found no association between FAM111A and other DNA-binding proteins from VACV or bacteria, further verifying that the interaction between FAM111A and I3 was specific. We also transfected FAM111A and I3 mRNA produced in RiboMAX™ large-scale

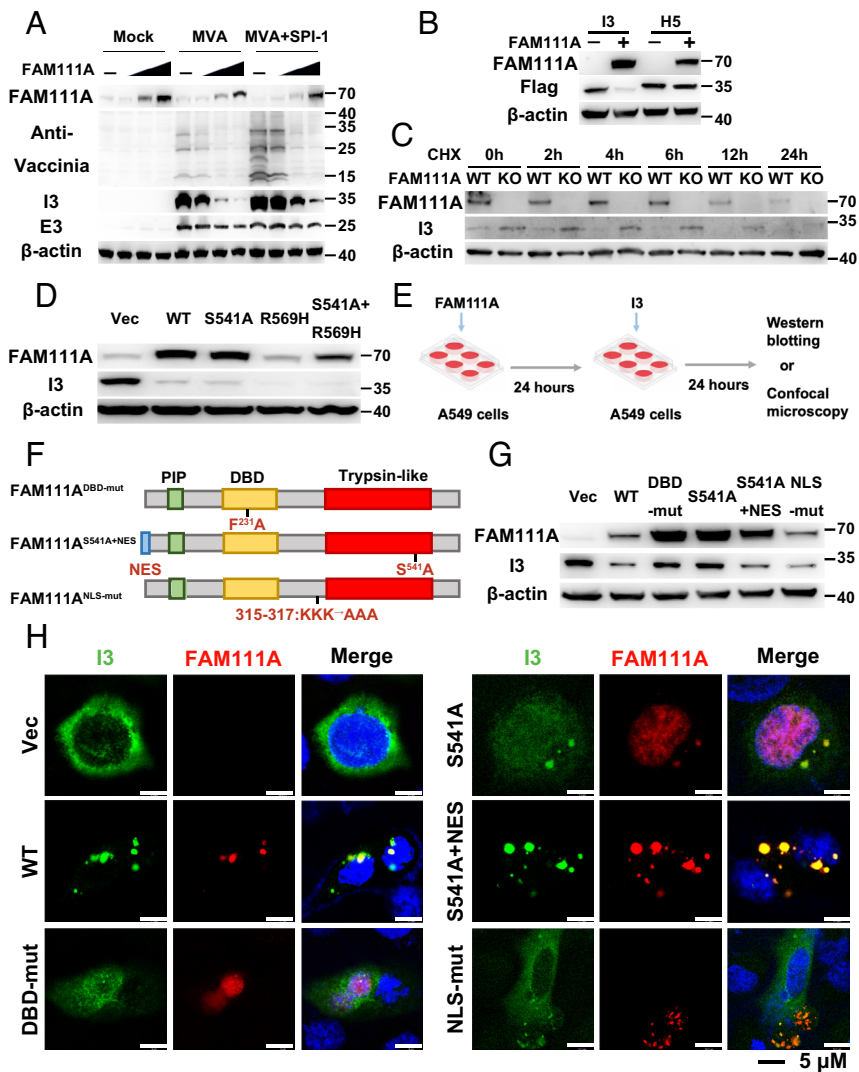


**Fig. 6.** Cytosolic FAM111A mediates protease-independent I3 degradation. (A) Human A549 cells were transfected with FAM111A at concentrations of 0.1, 0.5, and 1  $\mu\text{g}/\text{mL}$  for 24 h and infected with MVA or MVA+SPI-1 at 0.3 PFU/cell. Cell lysates were analyzed by SDS-PAGE and western blotting at 24 hpi. (B) Human A549 cells were cotransfected with flag-tagged I3 or H5 and FAM111A for 24 h. Cell lysates were analyzed by SDS-PAGE and western blotting. (C) Human A549<sup>WT</sup> or A549<sup>FAM111A-KO</sup> cells were transfected with I3 for 24 h before CHX was added. Cell lysates were analyzed by SDS-PAGE and western blotting 2 to 24 h after CHX was added. (D) Human A549 cells were cotransfected with VACV-I3 and FAM111A<sup>WT</sup> or lab-generated mutants indicated in Fig. 2A for 24 h. Cell lysates were analyzed by SDS-PAGE and western blotting. (E) Schematic flowchart of transfection experiments. Human A549 cells were transfected with FAM111A for 24 h before I3 transfection. After 24 h, cells were analyzed by western blotting or confocal microscopy. (F) Diagram of structures of FAM111A DBD mutant, FAM111A<sup>S541A</sup> mutant with nuclear export signal (NES), and FAM111A nuclear localization signal mutant (NLS-mut). (G) Human A549 cells were transfected with FAM111A<sup>WT</sup> and lab-generated mutants indicated in the figure for 24 h and then transfected with I3. After 24 h, cell lysates were analyzed by SDS-PAGE and western blotting. (H) Human A549 cells were transfected with FAM111A<sup>WT</sup> and indicated mutants for 24 h. Then indicated cells were transfected with VACV-I3. After 24 h, cells were then fixed, permeabilized, blocked, and stained with primary antibodies to I3 and FAM111A followed by fluorescent conjugated secondary antibodies. Hoechst was used to stain DNA. Scale bars are shown at the *Bottom*. Data in A–D, G, and H are representative of three independent experiments.

RNA production system and found no association between the two proteins, suggesting that plasmid DNA transfected was the source of DNA to bring FAM111A and I3 in close proximity (*SI Appendix, Fig. S8*). In summary, the specific association of FAM111A and I3 was shown by immunoaffinity purification and further suggested by their intracellular colocalization in the cytoplasm.

**FAM111A Promotes I3 Degradation without the Need of Its Protease Activity.** Next, experiments were performed to investigate whether FAM111A induced virus I3 degradation. A549 cells transfected with increasing amounts of FAM111A DNA were mock-infected or infected with MVA or MVA+SPI-1 at 3 PFU/cell, and viral protein synthesis was examined by western blotting analysis. Levels of I3 decreased as the amounts of FAM111A DNA transfected increased in infected cells (Fig. 6A). It is worth noting that FAM111A was also able to diminish I3 abundance in MVA+SPI-1-infected cells. One possible explanation is that the amount of SPI-1 present was not sufficient to fully restrict FAM111A when a high amount of FAM111A DNA was transfected. Nevertheless, it was apparent that I3 in MVA+SPI-1-infected cells was more resistant to FAM111A than that in MVA-infected cells (Fig. 6A). In comparison, E3, a viral early protein that binds dsRNA, was insensitive to FAM111A-promoted degradation (Fig. 6A). To further verify the specificity of I3 degradation by

FAM111A, we cotransfected A549 cells with DNAs encoding FAM111A and flag-tagged I3 or H5 and found that like E3, H5 was unaffected by FAM111A (Fig. 6B). To investigate whether the synthesis of VACV I3 was affected by FAM111A, we transfected A549<sup>WT</sup> or A549<sup>FAM111A-KO</sup> with VACV I3 DNA in the presence of cycloheximide (CHX), a protein translation inhibitor, and monitored the level of I3 at different time points. We found that the protein level of I3 was much lower in A549<sup>WT</sup> cells than in A549<sup>FAM111A-KO</sup> cells and remained in the A549<sup>FAM111A-KO</sup> cells until 12 h post CHX treatment, indicating that the decrease of VACV I3 was due to FAM111A-induced degradation rather than protein synthesis inhibition (Fig. 6C). These results demonstrated that FAM111A was specifically associated with VACV I3 and mediated its degradation upon virus infection.

To investigate whether FAM111A directly degrades I3 through its C-terminal protease activity, we simultaneously cotransfected A549 cells with I3 and FAM111A DNAs or its hyper- and hypoactive mutants and monitored protein levels of I3. Surprisingly, I3 was degraded when not only FAM111A<sup>WT</sup> DNA but also when FAM111A mutants with inactivated (FAM111A<sup>S541A</sup> and FAM111A<sup>S541A+R569H</sup>) protease activity were transfected (Fig. 6D). As we previously identified that the protease activity of FAM111A was crucial for its nuclear export, these combined results suggested that the FAM111A mutants with inactivated peptidase domain may bypass nuclear export and associate with I3 directly when

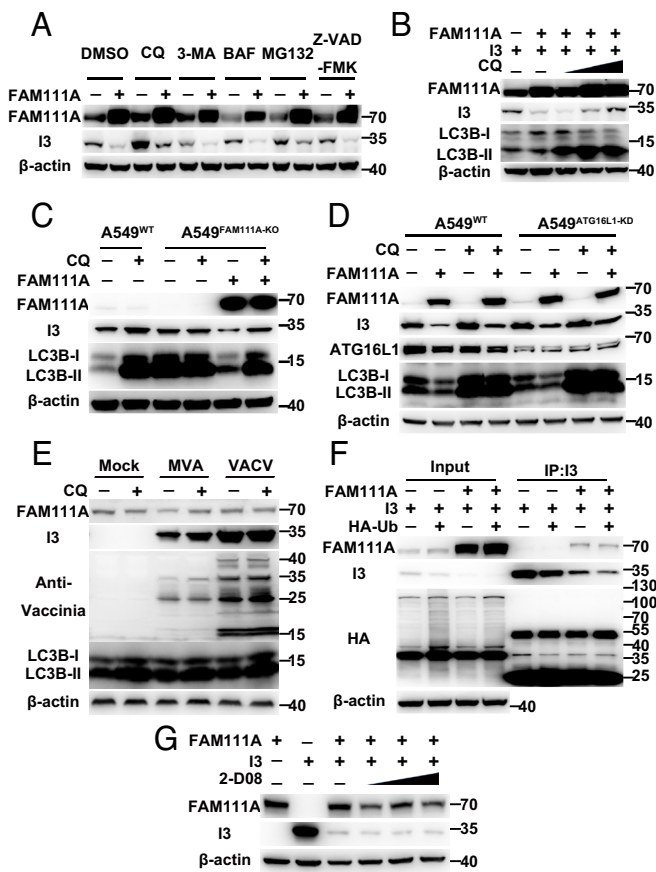


**Fig. 7.** FAM111A promotes I3 degradation through autophagy. (A) Human A549 cells were transfected with FAM111A for 24 h before transfecting with VACV-I3. Different drugs were added at the time of I3 transfection. After 24 h, cell lysates were analyzed by SDS-PAGE and western blotting. (B) Human A549 cells were transfected with FAM111A for 24 h before I3 transfection. CQ at various concentrations was added. After 24 h, cell lysates were analyzed by SDS-PAGE and western blotting. (C) Human A549<sup>WT</sup> or A549<sup>FAM111A-KO</sup> cells were transfected with FAM111A for 24 h before I3 was transfected and CQ added. After 24 h, cell lysates were analyzed by SDS-PAGE and western blotting. (D) Human A549<sup>WT</sup> or A549<sup>ATG16L1-KD</sup> cells were transfected with FAM111A for 24 h before I3 transfected. DMSO or CQ was added at the time of I3 transfection. After 24 h, cell lysates were analyzed by SDS-PAGE and western blotting. (E) Human A549 cells were infected with MVA or VACV-WR at 0.3 PFU/cell, and CQ was added at the time of infection. Cell lysates were analyzed by SDS-PAGE and western blotting at 8 hpi. (F) A549 cells were cotransfected with myc-tagged FAM111A, flag-tagged I3, and HA-tagged Ub for 24 h. Cell lysates were incubated with flag-conjugated beads at 4 °C for 18 h. Proteins were eluted with SDS-loading buffer and analyzed by SDS-PAGE and western blotting. The light chain or heavy chain antibody bands are at 25 kDa or 55 kDa, respectively. (G) Human A549 cells were transfected with FAM111A for 24 h before I3 transfection. 2-D08 at various concentrations was added. After 24 h, cell lysates were analyzed by SDS-PAGE and western blotting. Data in A–G are representative of three independent experiments.

they were coexpressed. The coexpression of FAM111A and I3 may lead to a premature association of FAM111A and I3 in the cytoplasm and result in I3 degradation. To test this hypothesis, we decided to alter our strategy by transfecting cells with FAM111A DNA or its derivative mutants for 24 h before transfecting I3. By doing this, FAM111A expressed could be localized to the correct subcellular compartments before interacting with I3 (Fig. 6E). In addition, we manipulated the subcellular localization of FAM111A by either attaching a nuclear export signal (NES) or disrupting its nuclear localization signal (NLS-mut) (Fig. 6F). A549 cells were transfected with FAM111A<sup>WT</sup>, FAM111A<sup>DBD-mutant</sup>, FAM111A<sup>S541A</sup>, FAM111A<sup>S541A+NES</sup>, or FAM111A<sup>NLS-mut</sup> DNAs for 24 h and then transfected with I3 DNA, and the levels of FAM111A and I3 were

examined by western blotting analysis. As expected, mutants with a disrupted dsDBD or inactivated protease domain lost their ability to degrade I3 (Fig. 6G) and were found primarily in the nucleus (Fig. 6H). Remarkably and interestingly, the mutant with an inactivated protease domain combined with an NES motif, which was found mostly in the cytosol, colocalized with I3 (Fig. 6H) and led to its degradation (Fig. 6G). Similarly, the mutant with a disrupted NLS was found primarily in the cytoplasm (Fig. 6H) and was also able to mediate I3 degradation. These results demonstrated that the catalytic function of FAM111A was only required for nuclear export but not I3 degradation.

**FAM111A Induces I3 Degradation through Autophagy.** Next, we explored the nature of I3 degradation by using a set of chemical inhibitors targeting various cellular pathways known to modulate protein degradation. A549 cells were sequentially transfected with FAM111A and I3 DNA (Fig. 6E) in the presence or absence of chemicals inhibiting autophagy [10 μM chloroquine (CQ), 5 mM 3-methyladenine (3-MA), and 0.5 μM bafilomycin A1 (BAF)], proteasomal degradation (20 μM MG132), or pancaspase activity (20 μM Z-VAD-FMK). While the addition of CQ and MG132 both alleviated FAM111A-induced degradation of I3, the addition of 3-MA, BAF or Z-VAD-FMK showed no discernible effects (Fig. 7A). We next performed a dose-dependent experiment and further confirmed that the addition of CQ caused the accumulation of LC3B-II and led to the rescue of FAM111A-mediated I3 degradation (Fig. 7B). Moreover, CQ slightly increased the expression I3 when cells were transfected with only I3 but not FAM111A (Fig. 7C), possibly due to I3 degradation stimulated by endogenous FAM111A, as this phenomenon was not observed in A549<sup>FAM111A-KO</sup> cells (Fig. 7C). To verify that the blockage of I3 degradation was not due to any off-target effect of CQ, we manipulated the level of ATG16L1, a key regulator of autophagic flow, by generating an A549 cell line in which the endogenous level of ATG16L1 was stably knocked down by shRNA and named the cell line A549<sup>ATG16L1-KD</sup> (Fig. 7D). Similar to the effect observed with CQ, depression of ATG16L1 was able to rescue FAM111A-mediated I3 degradation, suggesting the role of autophagy in such a process. To test whether FAM111A promoted I3 degradation during virus infection, we examined I3 abundance in the presence and absence of CQ upon virus infection. As shown in Fig. 7E, addition of CQ led to increased I3 expression during MVA but not VACV-WR infection (Fig. 7E). To rule out the participation of other protein-degradation pathways in I3 degradation, we examined whether FAM111A promoted ubiquitination of I3 and found I3 copurified with FAM111A exhibited no sign of ubiquitination (Fig. 7F). We also tested whether SUMOylation was involved by using a specific SUMOylation inhibitor 2-D08, and the results showed that the degradation of I3 was not recovered by pharmacologically inhibiting SUMOylation (Fig. 7G). The above results showed that FAM111A interacted with virus I3 and promoted I3 degradation by utilizing the autophagy pathway, rather than its protease activity.

**Poxvirus SPI-1 Blocks the Nuclear Export of FAM111A through Its Serpin Activity.** SPI-1 (C12 in VACV-cop) has previously been shown to function as a host range factor for MVA (19). To explore its role in FAM111A inhibition, we first observed its subcellular localization by infecting FAM111A-transfected A549 cells with MVA or MVA+SPI-1 at 3 PFU/cell and probed SPI-1 using a myc antibody at 12 hpi as the SPI-1 inserted into MVA contains a myc tag at its N terminus (19). The confocal microscopic analysis showed that SPI-1 was mainly localized in the nucleus during



MVA+SPI-1 infection (Fig. 8A). In addition, nuclear export of FAM111A activated by MVA was no longer observed when cells were infected with MVA+SPI-1 (Fig. 8B), suggesting that SPI-1 prevented FAM111A from exporting to the cytoplasm. To investigate whether SPI-1 was associated with FAM111A, we performed immunoprecipitation using either SPI-1 or FAM111A as the bait and observed a strong interaction between FAM111A and SPI-1 (Fig. 8C and D). We further verified that SPI-1 inhibited the destruction of NPCs by FAM111A after MVA infection using A549<sup>WT</sup> and A549<sup>FAM111A-KO</sup> cells. In A549<sup>WT</sup> cells, the expression level of NUP62 was significantly decreased when infected with MVA, while no significant change was observed in A549<sup>FAM111A-KO</sup> cells (Fig. 8E). The decreased level of NUP62 in cells infected with MVA+SPI-1 was lower than that of MVA, especially at 12 hpi (Fig. 8E). As FAM111A restricted viral replication by degrading virus I3, we next inspected whether SPI-1 could interfere with FAM111A-mediated I3 degradation. A549 cells were cotransfected with FAM111A, I3, and VACV-SPI-1 DNAs and proteins were harvested for western blotting analysis. Consistent with previous results, transfection of FAM111A DNA led to a prominent I3 degradation when SPI-1 was absent; however, this effect was alleviated when plasmid expressing VACV-SPI-1 was cotransfected (Fig. 8F). Interestingly, SPI-1 from MPXV, a close relative of VACV, and lumpy skin disease virus (LSDV), a member of the capripoxviruses, displaying 96.4% and 37.8% sequence identity with VACV SPI-1, respectively, could also inhibit FAM111A-mediated I3 degradation. A previous report identified cathepsin G as one of the cellular targets of rabbitpox virus SPI-1 and showed mutations in the RSL of SPI-1 abolished its interaction with cathepsin G (20). We thus introduced the two mutations T305R, F318A separately or in combination into VACV SPI-1 and examined their effects on FAM111A inhibition

(Fig. 8G). We used the same transfection strategy described in Fig. 6E by transfecting FAM111A DNA 24 h before transfecting I3 and SPI-1. As shown in Fig. 8G, wt-SPI-1 was able to rescue FAM111A-mediated I3 degradation; however, the SPI-1 with mutations in the RSL region failed to do so even though expressed at comparable levels compared to the wt-SPI-1. These results suggested that SPI-1 interacted with FAM111A via the RSL region and antagonized FAM111A's antiviral function by inhibiting the serine protease activity of FAM111A.

## Discussion

Our findings are summarized in a diagram presented in Fig. 9. FAM111A has been postulated to be a serine protease regulated in a cell cycle-dependent fashion and conserved in mammals (7). Recent studies showed FAM111A may restrict SV40 HR mutants and VACV infections (6, 8). We examined the effect of overexpressing or depressing FAM111A on virus replication using VACV that lacks a functional SPI-1 (VACV-ΔSPI-1) or MVA, which lost its SPI-1 during repeated passages in avian cells. Deletion of FAM111A with CRISPR-Cas9 or transient suppression with RNAi enhanced VACV-ΔSPI-1 or MVA replication in human A549 cells. In addition, we identified that its antiviral effect occurred postreplicative as a viral early gene E3 was expressed in the presence of FAM111A. Moreover, expression of FAM111A by transient transfection in human cells exhibited a strong inhibitory effect on viral DNA replication, viral protein expression, and virus replication, further confirming the antiviral function of FAM111A. The trypsin-like domain of FAM111A contains a catalytic triad including His385, Aps439, and Ser541 and a DBD that plays essential roles for its localization at the replication forks (5, 7, 28, 29). FAM111A was also shown to bind to the large T antigen of SV40 and inhibit the

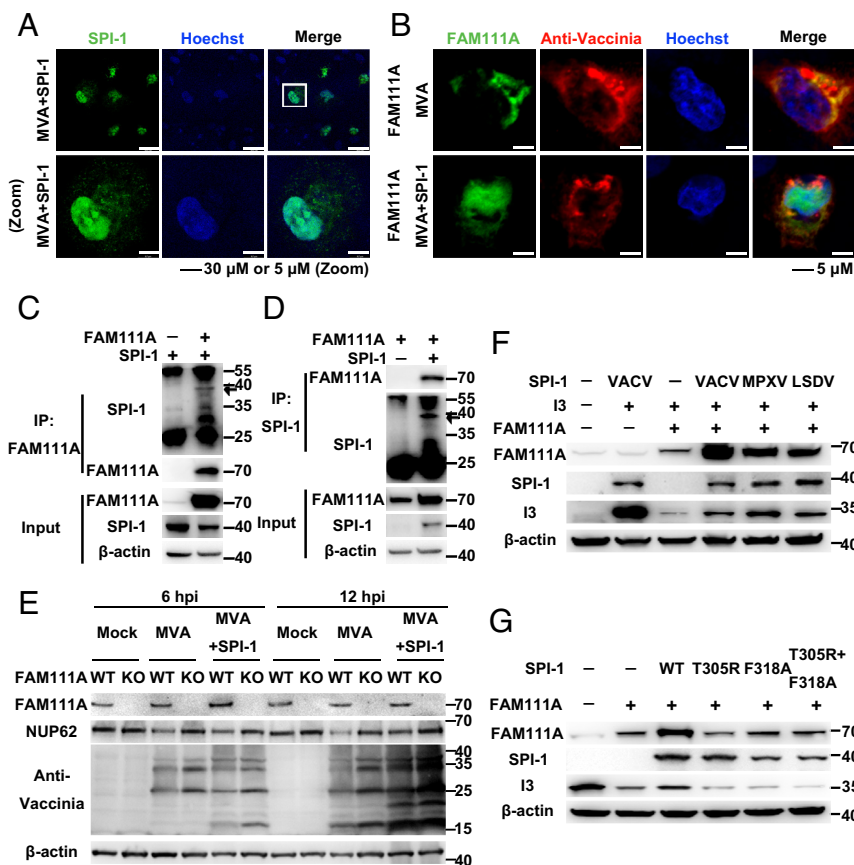


**Fig. 8.** Poxvirus SPI-1 antagonizes nuclear export of FAM111A and degradation of I3. (A) Human A549 cells were infected with MVA+SPI-1 at 3 PFU/cell. After 24 h, the cells were then fixed, permeabilized, blocked, and stained with primary antibodies to SPI-1 followed by fluorescent conjugated secondary antibodies. Hoechst was used to stain DNA. The scale bar is shown at the Bottom. (B) Human A549 cells were transfected with FAM111A for 24 h and then infected with MVA or MVA+SPI-1 at 3 PFU/cell. After 12 h, the cells were then fixed, permeabilized, blocked, and stained with primary antibodies to FAM111A and VACV followed by fluorescent conjugated secondary antibodies. Hoechst was used to stain DNA. The scale bar is shown at the Bottom. (C) Human A549<sup>WT</sup> or A549<sup>FAM111A-KO</sup> cells were infected with MVA or MVA+SPI-1 at 3 PFU/cell. Cell lysates were analyzed by SDS-PAGE and western blotting at 6 or 12 hpi. (D and E) Human A549 cells were cotransfected with myc-tagged FAM111A or flag-tagged SPI-1 for 24 h. Cell lysates were incubated with control magnetic beads or myc-/flag-conjugated beads at 4 °C for 18 h. Beads were extensively washed, and proteins were eluted with SDS-loading buffer and analyzed by SDS-PAGE and western blotting. The arrow indicates the correct band size for SPI-1, and the light chain or heavy chain antibody bands are at 25 kDa or 55 kDa, respectively. (F) Human A549 cells were cotransfected with flag-tagged SPI-1 of different viruses and a vector expressing FAM111A for 24 h before I3 transfection. After 24 h, cell lysates were analyzed by SDS-PAGE and western blotting. (G) Human A549 cells were cotransfected with flag-tagged SPI-1 of different mutants and a vector expressing FAM111A for 24 h. Then, indicated cells were infected with MVA at 0.3 PFU/cell. After 24 h, cell lysates were analyzed by SDS-PAGE and western blotting. Data in A–G are representative of three independent experiments.

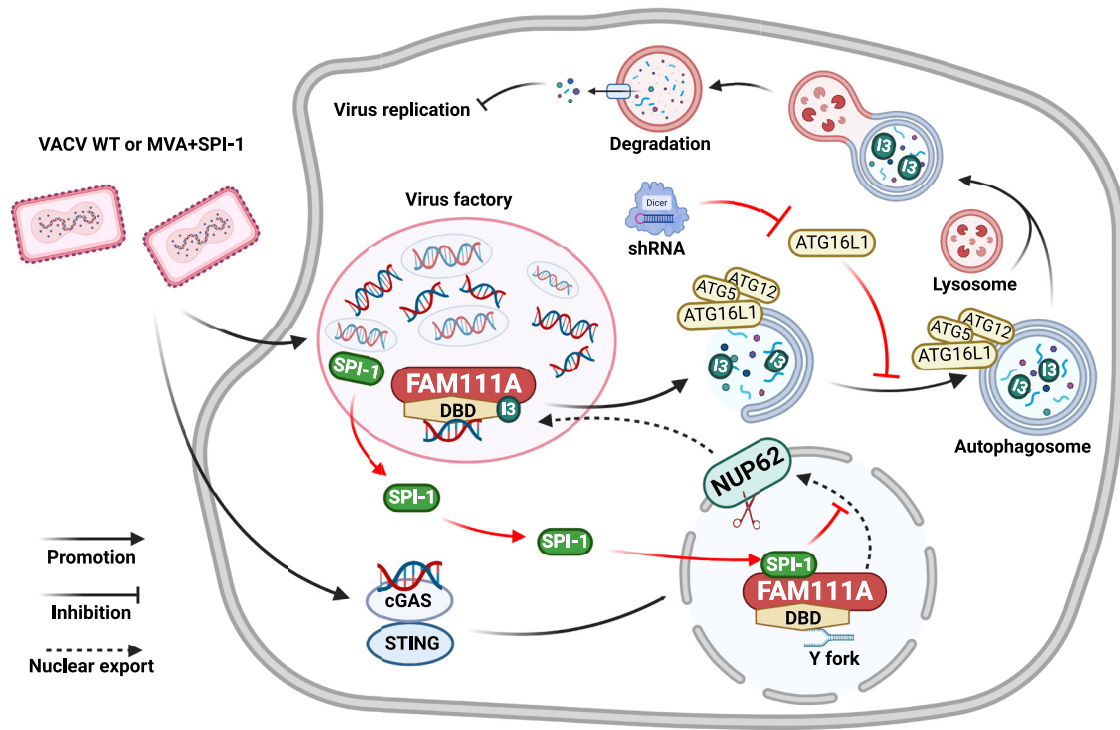


**Fig. 9.** FAM111A inhibits viral replication by inducing I3 degradation and is antagonized by VACV SPI-1. After SPI-1-deficient MVA or VACV invaded cells, the viral genomic DNA was recognized by the cGAS-STING signaling pathway, and its downstream signal activated nuclear export of FAM111A, allowing FAM111A in the nucleus to enter the cytoplasm by degrading the NPC. FAM111A is then recruited to the virus factory and binds to viral protein I3, which is thus degraded by autophagy. VACV SPI-1 enters the nucleus and inhibits the serine protease activity of FAM111A to prohibit its antiviral effect.

formation of the replication center of SV40 mutants (8). However, the replication of VACV differs from that of SV40 as the former completes its entire replication cycle in the cytoplasm of infected cells. As a result, nuclear export is the first step for FAM111A to confer its antiviral effect for VACV. Mutations of the catalytic triad of FAM111A abolished its antiviral activity for VACV- $\Delta$ SPI-1 and MVA as disruption of NPC no longer occurred (*SI Appendix, Fig. S6*). In addition, expression of FAM111A with an unmutated or hyperactive peptidase domain disrupted the nuclear membrane, which was previously reported and further demonstrated that the nuclear export of FAM111A upon infection is dependent on its peptidase activity (6). Following MVA infection, FAM111A translocated from the nucleus to the cytoplasm and colocalized with viral factories stained by Hoechst or I3 (Figs. 3 and 5). The change in FAM111A's subcellular localization relied on its DBD but not the PCNA-interaction motif. Another interesting question was how FAM111A, a protein exclusively found in the nucleus, senses VACV infection in the cytosol. Panda et al. postulated that replication factor C (RFC) 1-5 could load PCNA and may act as a DNA sensor recruiting FAM111A to viral genomes (10). Nonetheless, we found that mutations in the PCNA-interacting motif (FAM111A<sup>PCNA-mut</sup>) did not influence MVA restriction, suggesting that the recruitment of FAM111A to the viral factory is not PCNA mediated. Rather, mutations in the DBD abolished the nuclear export of FAM111A and resulted in its nuclear accumulation, indicating the involvement of DNA binding in FAM111A recruitment (Fig. 6). This was further validated by the findings that FAM111A<sup>DBD-mut</sup> no longer promoted I3 degradation.

Interestingly, the reduction of cGAS expression in cells inhibited the nuclear export of FAM111A, signifying the existence of a regulatory axis that associated the cGAS-STING signaling pathway with FAM111A (Fig. 4). Previous studies reported that POXIN encoded by VACV B2R was able to cleave 2',3'-cGAMP

and to antagonize the cGAS-STING signaling pathway. However, compared with VACV, the B2R ortholog encoded by MVA contains a premature stop codon due to mutations at the N-terminal end leading to a 186 a.a. deletion, which may seriously jeopardize its biological function (30). More needs to be done to clarify components in the cGAS-FAM111A regulatory pathway and to explore the nature of FAM111A activation upon virus infection. Previous studies showed that infection of an SV40 host range mutant enhanced the protease activity of FAM111A, leading to impairment of nuclear barrier function, cell morphology, and normal distribution of the nuclear pore (6). These results were in line with our observation, but the upstream activating signal for FAM111A may be different as SV40 replicates in the nucleus.

Using an immunoprecipitation assay coupled with mass spectrometry, we were able to identify the viral binding partners of FAM111A during MVA infection. We identified that cytosolic FAM111A interacted with viral I3 in a DNA-dependent manner. VACV I3 is a 34-kDa phosphoprotein essential for poxvirus genome replication. VACV- $\Delta$ I3 showed normal early gene expression and core disassembly but reduced DNA replication in non-complementing cells, a phenotype resembles that of FAM111A overexpression (27, 31). Like FAM111A, I3 can also bind DNA with its single-stranded DBD (SSB) (32). The interaction between FAM111A and I3 was terminated with benzonase treatment, but recovered when a protein cross-linker was added, and the FAM111A mutant that lacks a functional DBD no longer displayed any antiviral activity (Fig. 6). These observations highlight the importance of DNA-binding in its interaction with I3 and the recruitment of FAM111A to virus factories. Cytoplasmic FAM111A led to efficient I3 degradation, obstructing virus DNA replication and subsequent virus replication. Surprisingly, disease-associated mutations or loss-of-function mutations of

FAM111A did not influence its ability to promote I3 degradation as long as they were expressed in the cytoplasm. By manipulation of the subcellular localization of FAM111A using NES or interruption of NLS signals within FAM111A, we found that the catalytic activity of FAM111A was only required for nuclear export but not I3 degradation as the FAM111A<sup>S541A</sup> containing an NES (FAM111A<sup>S541A+NES</sup>) was still able to induce I3 degradation (Fig. 6G). Moreover, we found that the degradation of I3 by FAM111A did not rely on proteasomes, nor did it use the caspases. Instead, CQ treatment or depression of ATG16L1 by shRNA were both able to relax the degradation of I3 by FAM111A, demonstrating the role of autophagy in I3 degradation. In our assay, 3-MA and bafilomycin A1, two other inhibitors of autophagy, failed to negate FAM111A-mediated I3 degradation. The exact reason was unknown, but we speculated that it may be because bafilomycin A1, 3-MA, and chloroquine inhibit different steps of the autophagic flow and VACV may possess strategies to compensate for the blockade of autophagosome nucleation and lysosomal acidification, which were inhibited by 3-MA and bafilomycin A1, respectively (33).

VACV SPI-1 encoded by the C12 gene in RPXV was previously thought to affect the virus host range by inhibiting the serine protease activity of cathepsin G (20). VACV lacking SPI-1 exhibited low late and intermediate mRNAs but undiminished early mRNA (34). Deletion of SPI-1 did not affect virus virulence in a murine intranasal model (35). A more recent study confirmed the role of SPI-1 as a host range factor for the replication of MVA in mammalian cells (19). We found that SPI-1 mainly distributed in the nucleus after virus infection and interacted with FAM111A in a co-IP assay. The presence of SPI-1 was able to prevent FAM111A's nuclear export, thereby antagonizing its antiviral function. In RPXV, SPI-1 was predicted to be associated with viral proteins essential for DNA replication (36). Our results were in agreement with this hypothesis as we observed interactions and colocalization of SPI-1 and FAM111A within the nucleus of infected cells. Furthermore, we found that SPI-1 proteins from different orthopoxviruses (VACV and MPXV) and LSDV all inhibited FAM111A-mediated I3 degradation. Importantly, mutations of the two residues in the RSL of SPI-1 (T305R, F318A) abrogated its function in mitigating FAM111A-promoted I3 degradation without significantly affecting protein expression. As these two residues were previously reported to be essential for cathepsin G binding, we speculated that SPI-1 interacted with FAM111A via a similar region in its RSL (20).

Our work is a report of a mechanism by which FAM111A prohibited cytoplasmic DNA virus replication (summarized in Fig. 9). Our results indicated that nuclear components normally involved in mammalian cell DNA replication could translocate from the nucleus to the cytoplasm and restrict poxvirus replication by degrading key viral DNA replication-regulating protein I3 using the autophagic machinery. In addition, we presented an explanation for the immune evasion function of VACV SPI-1 in human cells.

## Materials and Methods

**Reagents.** A549 cells (ATCC CCL-185) were cultured in Dulbecco's Modified Eagle Medium (DMEM)/F-12. HeLa cells, 293T cells, and DF-1 cells were cultured in DMEM. BS-C-1 cells were cultured in Eagle's minimum essential medium. The commercial antibodies and chemicals are from various sources (i.e., Sigma-Aldrich, Thermo Fisher, Abcam, and Beyotime Biotechnology).

**Generation of Stable Cell Lines or Recombinant VACV.** The FAM111A-KO cell line was constructed using the CRISPR-Cas9 technology described previously (37). The A549-ATG16L1-KD cell line stably expressing ATG16L1-shRNA was constructed with retroviral transduction. Recombinant viruses were constructed by homologous recombination using fluorescent reporter genes (mCherry or eGFP) for plaque selection as previously described (37).

**Immunoprecipitation.** The treated cells were harvested 24 h posttransfection. Cells were lysed in wells with cell lysis buffer containing PMSF (Beyotime Biotechnology). Protein lysates were centrifuged for 15 min at 15,000 × g at 4 °C and then incubated with magnetic beads (Beyotime Biotechnology) at 4 °C for 8 h with rotation. The beads were washed and then subjected to SDS/PAGE and western blotting analysis.

**Quantitative PCR.** Total DNA was extracted with the DNeasy Blood/Tissue DNA mini kit (Qiagen), and the relative qPCR was performed with the Applied Biosystems SYBR Select Master Mix (Thermo Fisher) with gene-specific primers for virus E11 and host GAPDH as control. The results of virus genomic DNA were normalized to that of GAPDH, and relative DNA abundance was calculated.

**Immunofluorescence.** The treated cells on coverslips were fixed with 4% paraformaldehyde and permeabilized with 0.5% Triton X-100 in PBS. They were then incubated with proper primary antibodies in a humid chamber, followed by secondary antibodies. Nuclear DNA was stained with Hoechst. The cells were imaged using a Leica SP8 confocal microscope.

Detailed descriptions are provided in *SI Appendix, SI Materials and Methods*.

**Data, Materials, and Software Availability.** All study data are included in the main text and *SI Appendix*.

**ACKNOWLEDGMENTS.** This work was funded by the National Key Research and Development Program (2021YFD1800700), the National Natural Science Foundation of China (32172822), and the Beijing STRS program (Z211100002121021) to C.P. B.M. was supported by the Division of Intramural Research of the National Institute of Allergy and Infectious Diseases of the US NIH (1ZIAI000979-16).

Author affiliations: <sup>a</sup>National Key Laboratory of Veterinary Public Health and Safety, Key Laboratory of Animal Epidemiology of the Ministry of Agriculture and Rural Affairs, College of Veterinary Medicine, China Agricultural University, Beijing 100193, China; <sup>b</sup>Biotechnology Research Institute, Chinese Academy of Agricultural Sciences, Beijing 100081, China; <sup>c</sup>Agricultural Information Institute, Chinese Academy of Agricultural Sciences, Beijing 100081, China; and <sup>d</sup>Laboratory of Viral Diseases, National Institute of Allergy and Infectious Diseases, NIH, Bethesda, MD 20892

Author contributions: J.Z., B.M., and C.P. designed research; J.Z., X.G., Yijing Li, Z.Z., S.X., S.R., Yarui Li, H.L., K.N., S.F., Y.D., and Yinü Li performed research; Yijing Li, B.M., W.W., and C.P. contributed new reagents/analytic tools; J.Z., Yijing Li, Z.Z., S.X., B.M., W.W., and C.P. analyzed data; and J.Z. and C.P. wrote the paper.

1. L. Schelle, J. V. Corte-Real, P. J. Esteves, J. Abrantes, H. M. Baldauf, Functional cross-species conservation of guanylate-binding proteins in innate immunity. *Med. Microbiol. Immunol.* **212**, 141–152 (2023), 10.1007/s00430-022-00736-7.
2. J. P. Evans, S. L. Liu, Multifaceted roles of TIM-family proteins in virus-host interactions. *Trends Microbiol.* **28**, 224–235 (2020).
3. B. Wang, Y. P. Timilsena, E. Blanch, B. Adhikari, Lactoferrin: Structure, function, denaturation and digestion. *Crit. Rev. Food Sci. Nutr.* **59**, 580–596 (2019).
4. J. Y. Seo, R. Yaneva, P. Cresswell, Viperin: A multifunctional, interferon-inducible protein that regulates virus replication. *Cell Host Microbe* **10**, 534–539 (2011).
5. C. Alabert *et al.*, Nascent chromatin capture proteomics determines chromatin dynamics during DNA replication and identifies unknown fork components. *Nat. Cell Biol.* **16**, 281–293 (2014).
6. M. Nie *et al.*, FAM111A induces nuclear dysfunction in disease and viral restriction. *EMBO Rep.* **22**, e50803 (2021).

7. Y. Kojima *et al.*, FAM111A protects replication forks from protein obstacles via its trypsin-like domain. *Nat. Commun.* **11**, 1318 (2020).
8. R. M. Tarnita, A. R. Wilkie, J. A. DeCaprio, Contribution of DNA replication to the FAM111A-mediated Simian Virus 40 host range phenotype. *J. Virol.* **93**, e01330-18 (2019).
9. D. A. Fine *et al.*, Identification of FAM111A as an SV40 host range restriction and adenovirus helper factor. *PLoS Pathog.* **8**, e1002949 (2012).
10. D. Panda, D. J. Fernandez, M. Lal, E. Buehler, B. Moss, Triad of human cellular proteins, IRF2, FAM111A, and RFC3, restrict replication of orthopoxvirus SPI-1 host-range mutants. *Proc. Natl. Acad. Sci. U.S.A.* **114**, 3720–3725 (2017).
11. S. L. Haller, C. Peng, G. McFadden, S. Rothenburg, Poxviruses and the evolution of host range and virulence. *Infect. Genet. Evol.* **21**, 15–40 (2014).
12. H. Vauhkonen *et al.*, Intrahost monkeypox virus genome variation in patient with early infection, Finland, 2022. *Emerg. Infect. Dis.* **29**, 649–652 (2023).

13. R. M. Burdon *et al.*, Sustained Mpox proctitis with primary syphilis and HIV Seroconversion, Australia. *Emerg. Infect. Dis.* **29**, 647–649 (2023).
14. N. T. Dung *et al.*, Monkeypox virus infection in 2 female travelers returning to Vietnam from Dubai, United Arab Emirates, 2022. *Emerg. Infect. Dis.* **29**, 778–781 (2023).
15. A. M. McCollum *et al.*, Epidemiology of human Mpox–Worldwide, 2018–2021. *MMWR Morb. Mortal. Wkly Rep.* **72**, 68–72 (2023).
16. B. Moss, Genetically engineered poxviruses for recombinant gene expression, vaccination, and safety. *Proc. Natl. Acad. Sci. U.S.A.* **93**, 11341–11348 (1996).
17. E. Paoletti, Applications of pox virus vectors to vaccination: An update. *Proc. Natl. Acad. Sci. U.S.A.* **93**, 11349–11353 (1996).
18. A. Volz, G. Sutter, Modified vaccinia virus Ankara: History, value in basic research, and current perspectives for vaccine development. *Adv. Virus. Res.* **97**, 187–243 (2017).
19. R. Liu *et al.*, SPI-1 is a missing host-range factor required for replication of the attenuated modified vaccinia Ankara (MVA) vaccine vector in human cells. *PLoS Pathog.* **15**, e1007710 (2019).
20. K. B. Moon, P. C. Turner, R. W. Moyer, SPI-1-dependent host range of rabbitpox virus and complex formation with cathepsin G is associated with serpin motifs. *J. Virol.* **73**, 8999–9010 (1999).
21. C. Peng, B. Moss, Repair of a previously uncharacterized second host-range gene contributes to full replication of modified vaccinia virus Ankara (MVA) in human cells. *Proc. Natl. Acad. Sci. U.S.A.* **117**, 3759–3767 (2020).
22. J. L. Americo, P. L. Earl, B. Moss, Droplet digital PCR for rapid enumeration of viral genomes and particles from cells and animals infected with orthopoxviruses. *Virology* **511**, 19–22 (2017).
23. S. Unger *et al.*, FAM111A mutations result in hypoparathyroidism and impaired skeletal development. *Am. J. Hum. Genet.* **92**, 990–995 (2013).
24. T. S. Xiao, K. A. Fitzgerald, The cGAS-STING pathway for DNA sensing. *Mol. Cell* **51**, 135–139 (2013).
25. C. Chen, P. Xu, Cellular functions of cGAS-STING signaling. *Trends Cell Biol.* **3**, 630–648 (2022), 10.1016/j.tcb.2022.11.001.
26. M. L. Harrison, M. A. Desaulniers, R. S. Noyce, D. H. Evans, The acidic C-terminus of vaccinia virus I3 single-strand binding protein promotes proper assembly of DNA-protein complexes. *Virology* **489**, 212–222 (2016).
27. M. D. Greseth, M. W. Czamecki, M. S. Bluma, P. Traktman, Isolation and characterization of vDeltaI3 confirm that vaccinia virus SSB plays an essential role in viral replication. *J. Virol.* **92**, e01719-17 (2018).
28. A. L. Welter, Y. J. Machida, Functions and evolution of FAM111 serine proteases. *Front. Mol. Biosci.* **9**, 1081166 (2022).
29. A. Ruggiano, K. Ramadan, DNA-protein crosslink proteases in genome stability. *Commun. Biol.* **4**, 11 (2021).
30. J. B. Eaglesham, Y. Pan, T. S. Kupper, P. J. Kranzusch, Viral and metazoan poxins are cGAMP-specific nucleases that restrict cGAS-STING signalling. *Nature* **566**, 259–263 (2019).
31. T. G. Senkevich, G. C. Katsafanas, A. Weisberg, L. R. Olano, B. Moss, Identification of vaccinia virus replisome and transcriptome proteins by isolation of proteins on nascent DNA coupled with mass spectrometry. *J. Virol.* **91**, e01015-17 (2017).
32. M. Tseng, N. Palaniyar, W. Zhang, D. H. Evans, DNA binding and aggregation properties of the vaccinia virus I3L gene product. *J. Biol. Chem.* **274**, 21637–21644 (1999).
33. M. Mauthé *et al.*, Chloroquine inhibits autophagic flux by decreasing autophagosome-lysosome fusion. *Autophagy* **14**, 1435–1455 (2018).
34. J. L. Shisler, S. N. Isaacs, B. Moss, Vaccinia virus serpin-1 deletion mutant exhibits a host range defect characterized by low levels of intermediate and late mRNAs. *Virology* **262**, 298–311 (1999).
35. S. Kettle, N. W. Blake, K. M. Law, G. L. Smith, Vaccinia virus serpins B13R (SPI-2) and B22R (SPI-1) encode M(r) 38.5 and 40K, intracellular polypeptides that do not affect virus virulence in a murine intranasal model. *Virology* **206**, 136–147 (1995).
36. B. G. Luttge, R. W. Moyer, Suppressors of a host range mutation in the rabbitpox virus serpin SPI-1 map to proteins essential for viral DNA replication. *J. Virol.* **79**, 9168–9179 (2005).
37. C. Peng *et al.*, Zinc-finger antiviral protein (ZAP) is a restriction factor for replication of modified vaccinia virus Ankara (MVA) in human cells. *PLoS Pathog.* **16**, e1008845 (2020).